Available online at www.sciencedirect.com
ScienceDirect
Journal of the European Ceramic Society 31 (2011) 2593–2599
www.elsevier.com/locate/jeurceramsoc

Microstructural evolution of a commercial ultrafine alumina powder densified by different methods

Farhad Golestani-fard [a], Mehdi Mazaheri [b,*], Masoud Aminzare [a], T. Ebadzadeh [c]

[a] Department of Materials and Metallurgical Engineering, Iran University of Science and Technology, Tehran, Iran
[b] Institute of Physics of Complex Matter, Swiss Federal Institute of Technology Lausanne (EPFL), 1015 Lausanne, Switzerland
[c] Materials and Energy Research Center, Tehran, Iran

Available online 18 February 2011

Abstract

The densification and grain growth of bodies made from a commercial ultrafine alumina powder was investigated. The primary powder was initially subjected to dry (uniaxial cold pressing) and wet shaping (slip casting), followed by conventional (CS)-, two step (TSS)-, and microwave (MS) sintering to explore the effect of each series of treatments on the densification and microstructural evolution of the specimens. It was demonstrated that a uniform microstructure with higher density would be obtained using the wet shaping method. In addition, microwave sintering was found to be more effective into the densification of the specimens and in yielding a finer grain structure. It is believed that the high heating rate and effective particle packing are responsible for the improvements in these properties. On this basis, it was also demonstrated that the fracture toughness of the samples increased significantly through the application of microwave sintering.

Keywords: Sintering; Shaping; Grain size; Mechanical properties; Al_2O_3

1. Introduction

Most ceramic bodies are required to be sintered to a nearly full dense structure to meet the superiority of properties for structural applications. Therefore, a variety of approaches in the field of sintering have arisen due to the widespread demand of ceramics in recent decades. Hence, understanding how the processing variables affect microstructural evolution is the key to initiating a proper sintering procedure.[1,2] For example, some parameters, such as temperature, pressure, average particle size and atmosphere, must be controlled with adequate precision. Yet, other parameters such as the powder characteristics and particle packing, are hardly controllable but are still influential on the sintering process.

Different processing steps and variables are required to be considered for the manufacturing of samples with densities close to the theoretical value. For example, one may use variable methods in the shaping step, such as simple die compaction, isostatic pressing, slip casting and gel casting, based on the properties required for the final product. In light of shaping methods, not only the sintering conditions but also the sintered properties may differ noticeably. Krell and Klimke[3] shaped alumina nanopowder via different methods such as uniaxial pressing (UP), cold isostatic pressing (CIP), slip casting (SC) and gel casting (GC). They showed that densification was achievable at lower temperatures, provided that highly uniform packing could be attained in the green bodies. They demonstrated that conventional sintering of uniaxially pressed (UP) submicron alumina at 1450 °C was able to provide a relative density of ≈98% and a grain size of 1.25 μm.[4] The CIP bodies, sintered at 1400 °C, however, reached 99% density with a grain size of only 0.65 μm. The bodies also showed better mechanical properties, which were attributed to the higher compaction and the improved homogeneity of the particle coordination.[5] In addition, the activation energy of sintering for alumina nanopowder is highly dependent on the shape-forming technique. For example, the activation energy for pressure filtered (PF) and dry pressed (DP) alumina bodies were reported as 605 and 700 kJ/mol, respectively.[6,7] To explain this issue, we should mention that the forming method dictates the particle and pore arrangements. It also influences the contact between the particles, which directly affects the sinter ability. Therefore, the activation energy of the sintering process can be related to the shape-forming method, sintering conditions

* Corresponding author. Tel.: +41 21 693 3389; fax: +41 21 693 4470.
E-mail addresses: mehdi.mazaheri@epfl.ch, mmazaheri@gmail.com (M. Mazaheri).

0955-2219/$ – see front matter © 2010 Elsevier Ltd. All rights reserved.
doi:10.1016/j.jeurceramsoc.2010.12.022

Table 1
Purity and typical analysis of TM-DAR (as reported by the supplier).

Al_2O_3 (%)	Impurity (ppm)										
	Si	Fe	Na	K	Ca	Mg	Cu	Cr	Mn	U	Th
>99.99	10	8	8	3	3	2	1	<1	<1	<0.004	<0.005

and powder characterizations. For example, in wet shaping (e.g. pressure filtration) a high degree of ultrafine particle compaction lowers the activation energy.[6,7]

In addition, the various techniques employed through the sintering step can be the sources of inconsistencies in the properties of sintered nanostructures. Mazaheri et al.[8] densified pressed ZnO nanopowder (approximately 30 nm) by conventional pressureless sintering (CS) and hot pressing (HP) at 1200 and 800 °C, respectively. They demonstrated that the final grain size of nearly full dense samples manufactured by HP was 4 times smaller than that of the conventionally sintered samples. After the introduction of the two-step sintering (TSS) method by Chen and Wang,[9] many researchers applied this method to nanopowders. Mazaheri et al. have recently shown the effect of TSS on the structural evolution of nanocrystalline 8% YSZ,[10] 3% YSZ[11] and ZnO.[12] In the case of nanocrystalline 8% YSZ, a fine microstructure with a grain size of approximately 300 nm could be defined by the pinning effect of triple-point junctions through the second step of TSS, dragging the grain boundaries and, hence, contributing to a tangible grain-growth suppression.[9,10] Likewise, microwave sintering was reported as an additional resourceful technique for suppressing the grain growth and producing a homogenous microstructure.[13]

In the present study, nanocrystalline alumina powder has been subjected to the shaping methods of UP and SC to highlight the significance of the consolidation technique. Additionally, to understand the effect of the green state on the sintering path and mechanical properties of sintered bodies, the microstructural evolution was investigated. Moreover, microwave heating and two-step sintering were applied on some samples to explore the effect of the sintering technique on the grain growth.

2. Experimental procedures

2.1. Fabrication of the green bodies

The alumina powder (Taimicron TM-DAR; Taimei Chemicals Co., Ltd., Tokyo, Japan (Table 1)) was shaped using two different methods: DP and SC. Uniaxial pressing was performed in a steel cylindrical die (10 mm in diameter) through pressures ranging from 50 to 900 MPa. The green pellets were characterized by density measurements using the volumetric method. An accurate balance (10^{-4} g) and a micrometer calliper (10^{-4} m) were used for determining the weight and dimensions of the bodies. The SC specimens were produced by providing aqueous slurries with different solid contents (45–75 wt%) mixed with a constant amount (0.8 wt% solid) of Dolapix (CE64, Zschimmer & Schwarz, Lahnstein, Germany) as a sterical stabilizer of the slurry.[3,4] Mercury porosimetry was then used to study the pore-size distribution of the green bodies prepared by SC and DP methods. To avoid sample fracture during the porosimetry test in mercury, pre-sintering was performed by heating the green bodies at 900 °C.

2.2. Sintering

To investigate the effect of the shaping method on the densification behavior of the samples, green bodies formed via DP and SC methods were conventionally sintered with a heating rate of 10 °C min^{-1} up to 1550 °C without soaking time. The effect of the sintering technique was explored by heating the specimens of the highest relative green density (≈56% TD, pressed at 600 MPa) under the microwave and TSS conditions. Microwave sintering (MS) was conducted in a domestic microwave oven with 900 W of power and a 2.45 GHz microwave cavity (Fig. 1). Alumina exhibits low dielectric loss (0.1 ± 0.03) and is difficult to heat in a microwave furnace at room temperature; hence, a SiC crucible with a high dielectric loss (300 ± 50) was employed as a susceptor. The temperature measurements were performed using an optical pyrometer (Model: RAYR312MSCL2G) focused through a hole in the top of the insulation on the surface of the sample.[14] The microwave-sintered samples were heated to 1450 °C with an approximately higher heating rate of 30 °C min^{-1}.

TSS, alternatively, was conducted via heating to 1250 °C with no holding time, followed by cooling to 1050 °C with extended soaking times. The densification behavior of the present powder using TSS has been reported previously.[15] The density of the sintered pellets was measured using the Archimedes method.

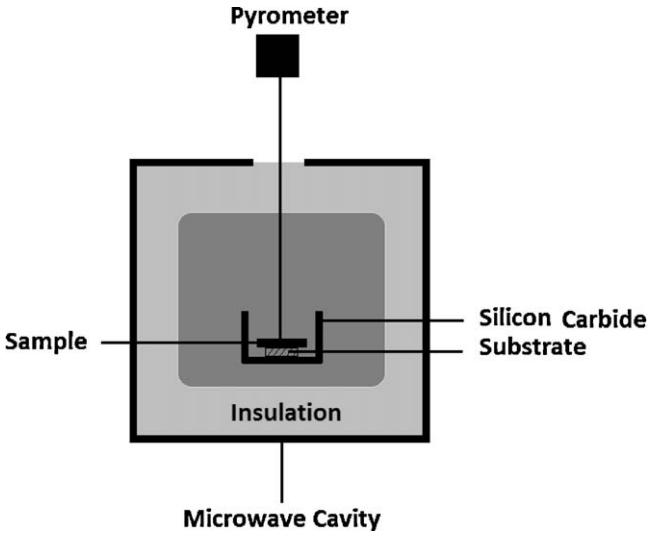

Fig. 1. Schematic diagram of the microwave system.

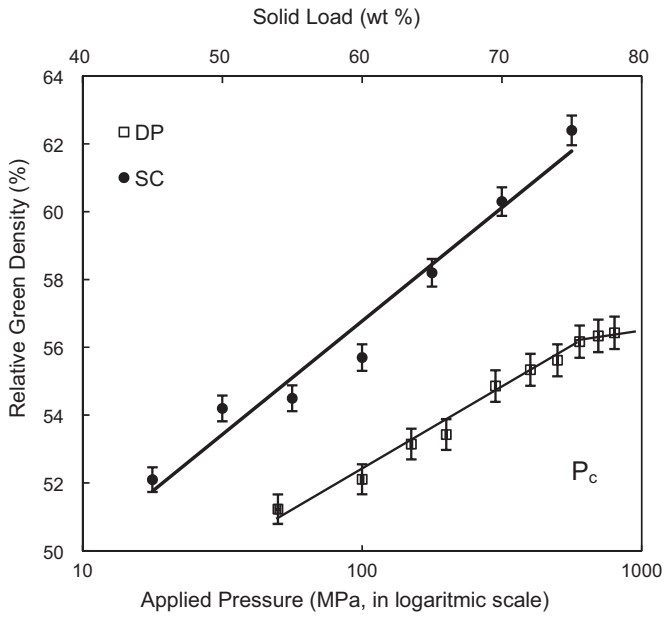

Fig. 2. The effect of the applied pressure and solid load on the relative green density of the alumina bodies shaped by DP and SC, respectively.

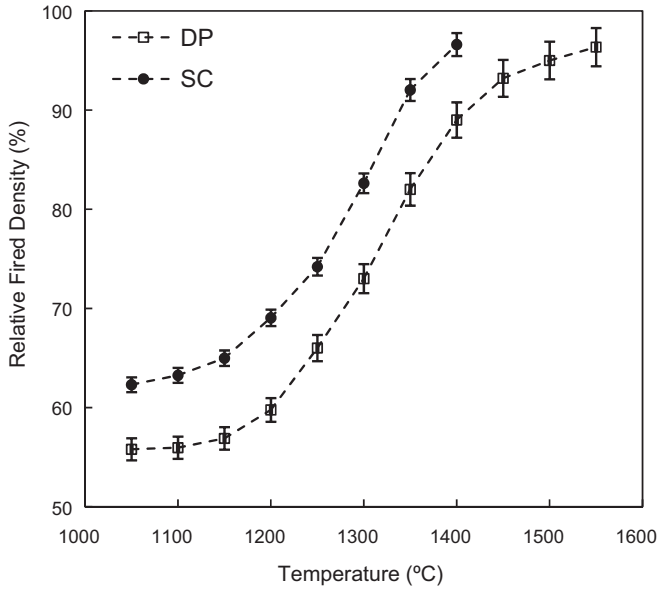

Fig. 3. The relationship between the relative fired density and sintering temperature for DP and SC bodies conventionally sintered up to 1550 °C with a constant heating rate of 10 °C min^{-1}. The samples with a green density of 63% TD for the SC bodies and 55% TD for the DP bodies were utilized.

The microstructures of the specimens were studied using Scanning Electron Microscopy (SEM, Philips XL30). The grain size of the sintered samples was calculated using an image analyzer, and the average values were reported.

2.3. Mechanical properties

The hardness and fracture toughness measurements were performed by applying indentation and measuring the crack length (Buehler, MTX-AL, Germany), according to ASTM C1327. The indentation tests were performed on polished samples with a load of 10 kg held for 20 s. At least 3 indentations from different places on the surface of the specimens performed then, these indentations were used to calculate the fracture toughness (FT). Details of the hardness and fracture toughness calculations can be found in our previousarticles.[6,15]

3. Results and discussion

3.1. The effect of the fabrication method

Fig. 2 shows the relative green density of DP and SC bodies as a function of the applied pressure (on a logarithmic scale) and solid load (wt%), respectively. As can be observed, the solid-content increase results in a gradual rise in the green density in the SC specimens. The graph representing the behavior of the dry-pressed samples, however, shows a break point where the green density reaches 55% TD, or a pressure of 600 MPa. It is also clear that the compaction of the SC bodies is always better than the DP samples. While inspecting the green bodies, the formation of laminated layers transverse to the load direction at high pressures (e.g., 900 MPa) was observed. Mazaheri et al.[16] attributed the two break points in the green density–pressure graph to agglomerates strength and to the decline in the compaction after the particle rearrangement. The presence of a single break point at 600 MPa is evidence that the present alumina powder is non-agglomerated.

As shown in Fig. 2, the SC specimens with a solid load of ≈75 wt% can reach a density of above 62% TD. It is also interesting that the SC bodies have demonstrated generally higher green densities compared to their dry-pressed counterparts. These facts imply that the particles have the opportunity to rearrange and slide over each other freely during slip casting; therefore, wet shaping methods provide particles with suitable freedom to find their optimum positions on their own.

On the contrary, the external forces through dry pressing can hardly move an individual particle into the voids available.[3,4] Thus, in the DP process, the uniform packing of powders demands extremely high pressures to overcome the huge forces rising from the particles' friction. The wet shaping processes, however, provide enough freedom for the particles to find a convenient position on their own.

Fig. 3 shows the fractional fired density of SC samples with a solid load of 75 wt% and DP sample at 600 MPa, both having the highest green densities. As can be observed, both pressed and SC specimens represent a typical sintering curve with a sigmoidal shape. Through the initial stage of sintering, the DP specimens undergo a slight density increment below 1200 °C. However, the rate of sintering demonstrates a remarkable rise between 1200 and 1400 °C up to the fractional density of 90% TD due to entering the final stage of sintering. A further increase in temperature from 1400 to 1550 °C results in a minor density enhancement of approximately 6% TD (from 90% to 96% TD). A slow sintering rate at the final stage (TD > 90%) is interpreted by the insoluble gas pressure trapped in the residual pores, suppressing the diffusional densification mechanisms.[12,17]

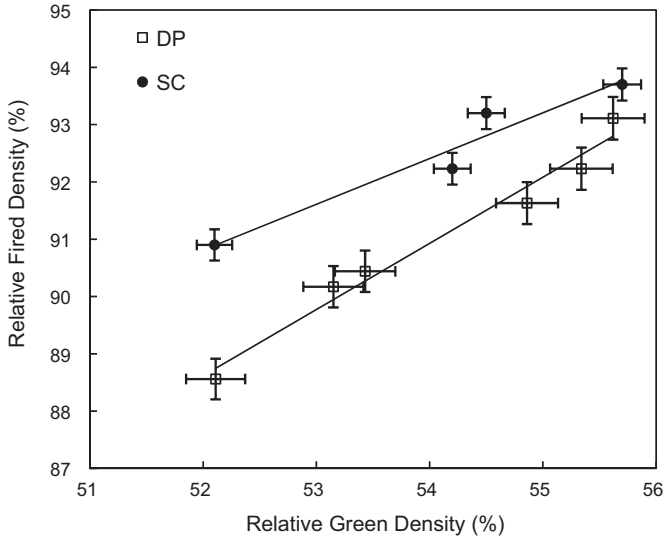

Fig. 4. The fractional fired density as a function of the fractional green density for the DP and SC samples. All of the samples were sintered with a heating rate of 10 °C min^{-1} up to 1400 °C.

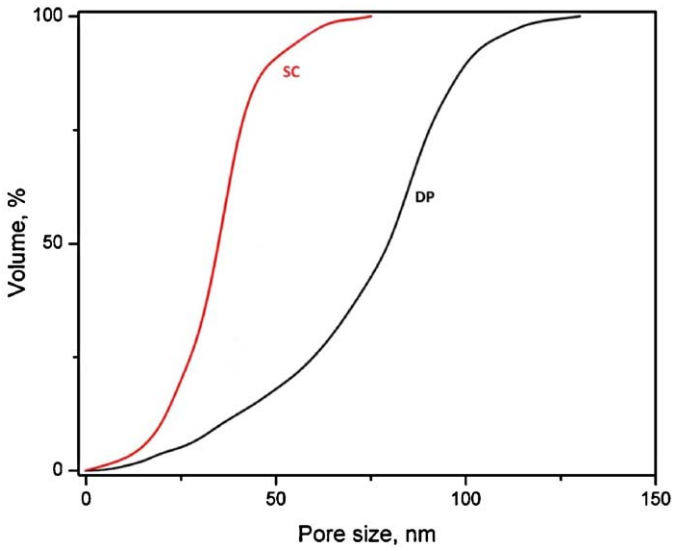

Fig. 5. The pore-size distribution of the alumina compacts shaped by DP (pressed at 400 MPa) and SC (with a solid load of 60 wt%). Both samples have an identical green density of ≈55% TD and were pre-sintered at 900 °C.

On the other hand, the SC bodies show significantly higher fractional fired densities compared to the pressed compacts sintered at equivalent temperatures. For instance, while soaking the SC specimens at 1250 °C gave rise to a fired density of 74% TD, the dry-pressed samples could only be densified to 65% TD. Referring to the literature[3] and present results (Fig. 2), the higher green density of the SC bodies can be attributed to the homogenous particle arrangement facilitated by wet the shaping methods. This factor plays a key role in the better densification behavior compared to the conventional pressed samples, in which the packing usually suffers from homogeneity. Therefore, a lower sintering temperature (e.g., 150 °C lower) is needed for a SC sample to have a final density equal to that of a DP compact.

Fig. 4 shows the fractional fired density of the DP samples and SC bodies as a function of the fractional green density. The figure reveals that the SC bodies enjoy a higher sinterability compared to DP samples at even identical green densities. To exclude the effect of green density on the densification, the specimens prepared by both wet and dry methods with the same green density of ∼55% TD were subjected to a porosimetry experiment. The accumulated pore-size distributions of the bodies prepared by DP (at 400 MPa) and SC (with a solid load of 60 wt%) are compared in Fig. 5, and two distinguished differences can be highlighted from the porosimetery result. First, pores up to 130 nm in DP samples can be observed, while in the SC bodies, the largest pore detected is approximately 75 nm. Second, the pore-size distribution in the SC bodies is significantly narrower than in the DP samples. The wider pore-size distribution of the DP samples originates from the agglomerates of individual particles and represents a poor general homogeneity of the particle coordination.[3–5] The existence of larger pores through the green bodies promotes the inhomogeneous local shrinkage in subsequent sintering and, hence, leads to the higher sintering temperature for DP samples, as explained previously. In contrast, the higher slope in the pore-size distribution graph (smaller pore size) of the SC bodies implies a smaller pore size (down to the nanoscale) and consequently, an improved homogeneity for the SC nanostructures. Fig. 6 shows the typical SEM micrographs of DP and SC compacts after being sintered at 1550 and 1400 °C, respectively. While the average grain size of the

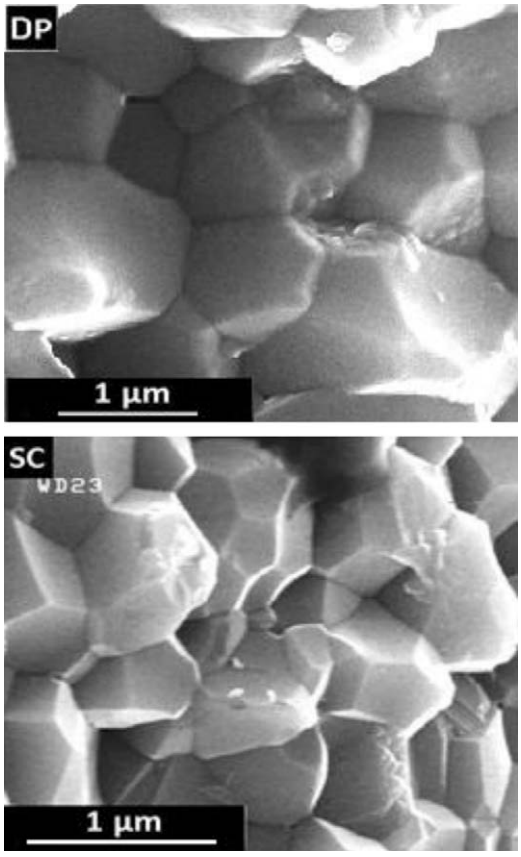

Fig. 6. The microstructure of the alumina bodies shaped by DP and SC after conventional sintering at 1550 and 1400 °C, respectively, with a heating rate of 10 °C min^{-1}.

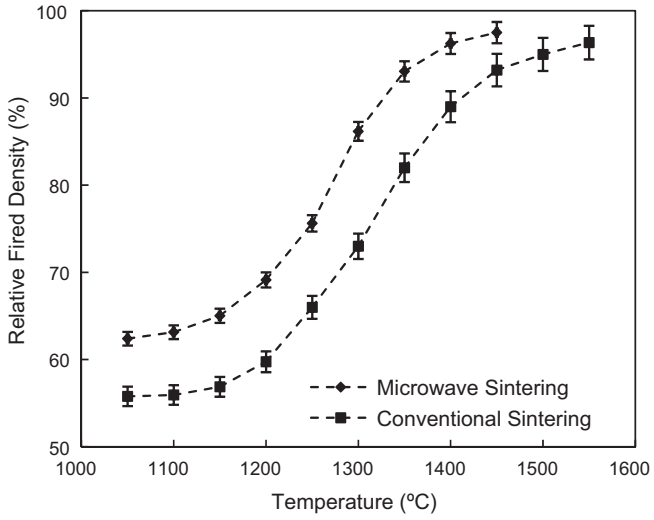

Fig. 7. The fractional fired density of DP alumina sintered via the conventional and microwave methods with heating rates of 10 and 30 °C min^{-1}, respectively.

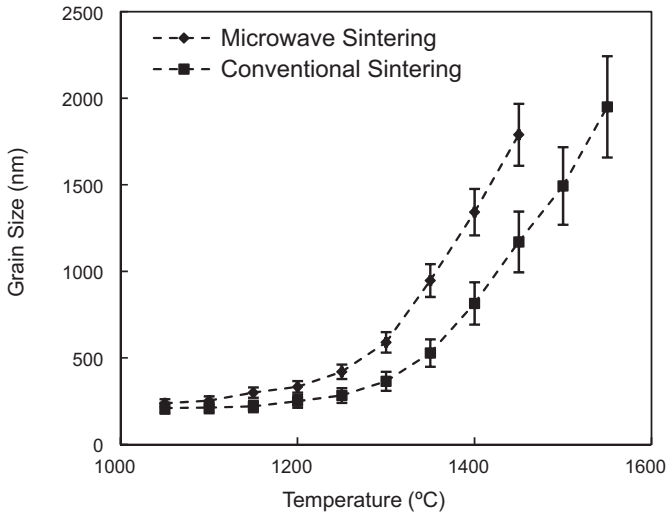

Fig. 8. The grain size as a function of the sintering temperature for DP alumina sintered by CS and MS sintering.

DP sample is approximately 1.95 μm, the wet-shaped alumina body yields a finer texture of ~1.5 μm.

3.2. The Effect of the sintering technique

Fig. 7 shows the effect of the applied sintering technique (CS versus MS) on the densification process of pressed alumina powder as a function of the sintering temperature. Both densification curves illustrate a sigmoidal shape, yet a meaningful difference between the fractional fired densities of the conventionally sintered samples and those prepared by microwave heating can be observed. According to previous reports,[18–20] microwave heating has been recognized as a promising method to improve the densification in the same ceramic systems. The sintering path of microwave-heated specimens typically shifts to higher densities, mainly near 96% TD.[13] This may be attributed to the potential of microwaves to provide higher densities at lower temperatures compared to CS densification. However, the densification and microstructural evolution of MS ceramic bodies require additional studies.

Fig. 8 shows the grain-size variation of CS and MS specimens versus the sintering temperature. It is worth to mentioning that the average grain size of the MS specimens appears higher for any given temperature with respect to the CS samples. However, as shown in Fig. 7, the higher heating rate related to the MS procedure has resulted in a higher density compared to conventionally sintered samples. In other words, fast firing in this method generates a higher densification at each temperature compared to the CS method. Therefore, it is not appropriate to compare the grain sizes of the CS and MS samples if the sample densities are ignored. Hence, the sintering path (i.e. grain size versus sintered specimen density) could draw a more in depth comparison between the different sintering techniques (Fig. 9). It can be seen in Fig. 9 that the average grain size of the microwave-fired samples is lower than 1.75 μm compared to 1.95 μm for the CS samples.

Fig. 9 shows the influence of the formation and the sintering methods on the densification behavior and grain growth of the bodies prepared by SC and DP techniques and with the maximum obtainable green density in each class. The results of the DP bodies sintered via microwave heating and the two-step sintering methods were also added. As shown, all the conventionally sintered specimens experienced a typical exaggerated grain growth in the final stage of sintering (TD ~ 90%) regardless of the shaping method. However, it is worth to noting the moderate trend of parabolic grain growth in the SC bodies compared to the DP bodies.

Although the advantage of a wet shaping method, such as SC, caused an enhancement in the densification kinetics (Figs. 3 and 4), the grain growth tendency is not much influenced by the employed conformation method. Moreover, the effect of the conformation method on the sintering parameters can be more stimulated for the systems in which the ratio of the

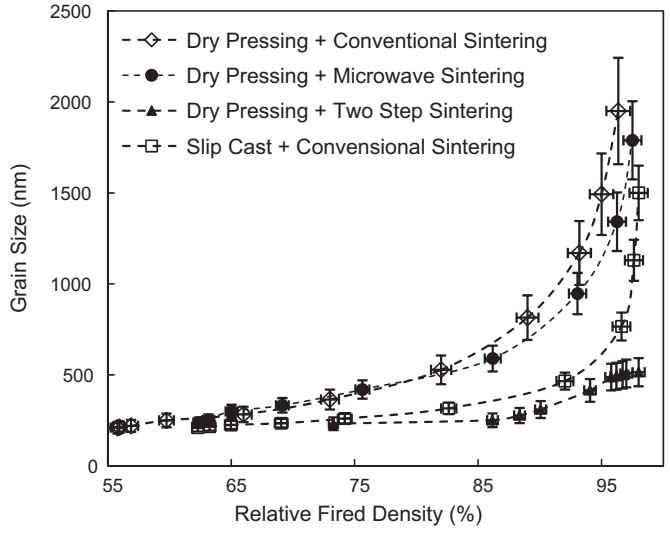

Fig. 9. The effect of the different shaping methods and sintering techniques on the sintering paths of alumina compacts. Two-step sintering and microwave heating were performed on the green samples formed by DP.

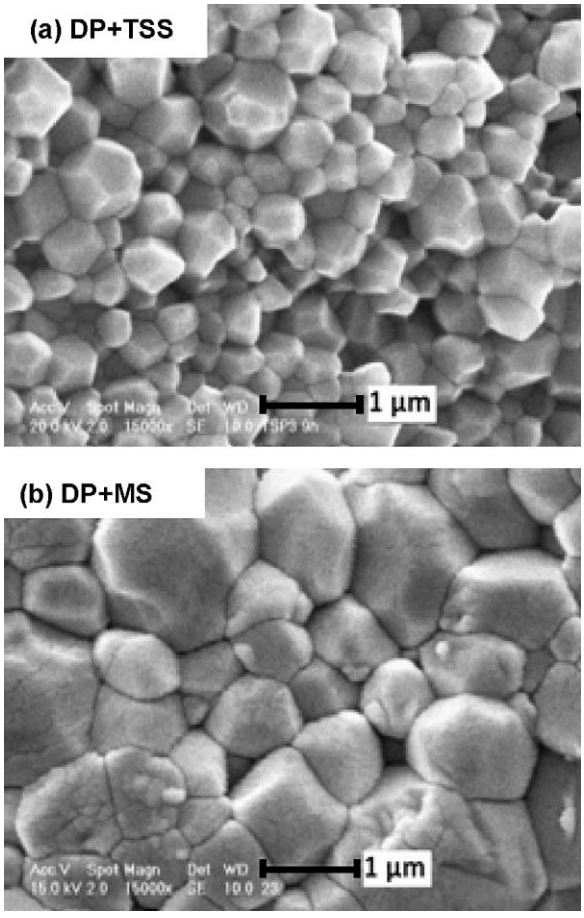

Fig. 10. SEM micrograph of nearly full dense DP samples sintered under (a) TSS and (b) MS techniques.

grain growth relative to the densification rate adopts higher values (i.e., dry pressing; Fig. 9). As the densification rate of the SC green bodies is due to the higher green density and finer residual pores (Fig. 5), a decrease in the sintering temperature and sintering time can be expected (Fig. 3). This, of course, will be accompanied by adequate significant grain growth suppression (Fig. 9). On this basis the sintering temperature of the SC bodies was found to be 150 °C lower than that of the DP compacts.

As presented in previous publications[10,12,21] the efficiency of the TSS method for controlling the grain growth during densification at the final stage of sintering is significant. As shown in Figs. 9 and 10(a), no parabolic growth was observed in the TSS graph. This finding refers to the lower temperature in the second step of TSS, at which the immobile triple-point junctions pin the grain boundaries and lead to the suppression of the grain growth, while the densification mechanisms, such the grain boundary diffusion, are active.[9] The MS micrograph (Figs. 9 and 10(b)), on the other hand, demonstrates a trend similar to the one for conventionally sintered SC bodies. The shorter sintering time and the fast firing in the MS procedure has led to an improved densification rate compared to the grain growth.

3.3. Hardness and fracture toughness

The hardness and fracture toughness (FT) of nearly full dense samples are summarized in Table 2. As seen in the table, no significant change in hardness can be related to the grain-size variation. Based on the present results, the final density of the specimens and, consequently, the available porosity of the nanostructured materials are the most effective criteria for the final values of the hardness and FT.[15,22] The minimum hardness of the dry-pressed samples, among other specimens subjected to different fabrication methods, is proper evidence for such a claim. The hardness range of the specimens (16.78–18.31 GPa) produced through different methods in the present study is close to the available results addressed by other investigators.[3–5,15] The results show that the hardness of the sintered samples does not strongly depend on the grain size. As can be observed in Table 2, the FT ranges from 2.41 (for CS) to 4.29 MPa $m^{1/2}$ (for TSS). The slip casting led to a FT value that is almost expected from TSS- or MS-derived samples. For TSS samples, this behavior can be attributed to the microstructure refining: a well-known mechanism for enhancing the mechanical properties of ceramic bodies.[10,12,15,22] The finer microstructures contain a higher volume of grain boundaries and are effective obstacles against the deformation. The difference between the FT of the nearly full dense bodies sintered through TSS and CS could be referred to as microstructural refining. This issue, however, requires further investigations on the microstructure of the bodies.

Table 2
Mechanical properties of nearly full dense alumina specimens processed via different methods.

Processing method	Relative density (%)	Grain size (μm)	Hardness (GPa)	Fracture toughness (MPa $m^{1/2}$)
CS[a]	96.3	1.95	16.78 ± 0.32	2.41 ± 0.15
SC[b]	97.8	1.5	18.19 ± 0.24	3.33 ± 0.13
TSS[c]	98	0.515	18.04 ± 0.19	4.29 ± 0.09
MS[d]	97.5	1.78	18.31 ± 0.21	3.22 ± 0.12

[a] Dry pressing + conventional sintering.
[b] Slip casting + conventional sintering.
[c] Dry pressing + two step sintering.
[d] Dry pressing + microwave sintering.

Based on the present results, the only definite conclusion is that the grain-size reduction of the CS and SC bodies from 1.95 to 1.5 μm, respectively, accompanied by the higher homogeneity of the SC green bodies along with small residual pores, is responsible for the enhancement in the FT of the SC bodies. This conclusion is supported by previous studies, in which such a particle-size distribution was reported as the underlying reason for the lower shrinkage.[3,5] The authors have previously hypothesized with the same scenario (higher microstructural homogeneity) for the higher FT of the microwave-sintered 8% YSZ samples.[13]

4. Conclusion

The microstructural evolution of the ultrafine alumina powder subjected to variable shaping methods (DP and SC) followed by different sintering techniques (CS, TSS and MS), has been detected in the current investigation. A summary of the consequences includes the following:

(1) The slip casting as a wet shaping method a more successful method in deriving nanostructures with a higher green density. While the maximum accessible green density of dry-pressed (at 600 MPa) samples was measured as 56% TD, the SC specimens (containing 75 wt% alumina powder) demonstrated a green density of approximately 64% TD.
(2) The SC samples, due to the finer pores (75 versus 135 nm) and narrower size distribution, display a higher green density than the DP compacts and, therefore, could be sintered at a lower temperature. Due to the larger grain size and lower density of the DP specimens (96.3% TD, 1.95 μm) compared to the finer grains in the SC bodies (97.8% TD, 1.5 μm), the DP samples demonstrated inferior mechanical properties.
(3) Nearly full dense bodies with grain sizes of ∼500 nm were attained by the TSS method, while the MS method yielded full dense bodies with average grain sizes of ≈1.78 μm. The hardness and FT of these bodies, however, did not vary considerably.

References

1. Kang S-JL. *Sintering*. 1st ed. London: Elsevier Butterworth-Heinemann; 2005.
2. Rahaman MN. *Ceramic processing and sintering*. 2nd ed. New York: CRC Press; 2003.
3. Krell A, Klimke J. Effects of the homogeneity of particle coordination on solid-state sintering of transparent alumina. *J Am Ceram Soc* 2006;**89**(6):1985–92.
4. Krell A, Blank P. The influence of shaping method on the grain size dependence of strength in dense submicrometre alumina. *J Eur Ceram Soc* 1996;**16**(11):1189–200.
5. Krell A, Blank P, Ma H, Hutzler T, Nebelung M. Processing of high-density submicrometer Al_2O_3 for new applications. *J Am Ceram Soc* 2003;**86**(4):546–53.
6. Aminzare M, Golestani-fard F, Guillon O, Mazaheri M, Rezaie HR. Sintering behavior of an ultrafine alumina powder shaped by pressure filtration and dry pressing. *Mater Sci Eng A* 2010;**527**:3807–12.
7. Aminzare M, Mazaheri M, Golestani-fard F, Rezaie HR, Ejeian R. Sintering behavior of nano alumina powder shaped by pressure filtration. *Ceram Int* 2011;**37**(1):9–14.
8. Mazaheri M, Hassanzadeh-Tabrizi SA, Sadrnezhaad SK. Hot pressing of nanocrystalline zinc oxide compacts: densification and grain growth during sintering. *Ceram Int* 2009;**35**:991–5.
9. Chen IW, Wang XH. Sintering dense nanocrystalline oxide with-out final stage grain growth. *Nature* 2000;**404**:168–71.
10. Mazaheri M, Valefi M, Hesabi ZR, Sadrnezhaad SK. Two-step sintering of nanocrystalline $8Y_2O_3$ stabilized ZrO_2 synthesized by glycine nitrate. *Ceram Int* 2009;**35**(1):13–20.
11. Mazaheri M, Simchi A, Golestani-Fard F. Densification and grain growth of nanocrystalline 3Y-TZP during two-step sintering. *J Eur Ceram Soc* 2008;**28**:2933–9.
12. Mazaheri M, Zahedi AM, Sadrnezhaad SK. Two-step sintering of nanocrystalline ZnO compacts: effect of temperature on densification and grain growth. *J Am Ceram Soc* 2008;**91**(1):56–63.
13. Mazaheri M, Zahedi AM, Hejazi M. Processing of nanocrystalline 8 mol% yttria-stabilized zirconia by conventional, microwave-assisted and two-step sintering. *Mater Sci Eng A* 2008;**492**:261–7.
14. Ebadzadeh T, Sarrafi MH, Salahi E. Microwave-assisted synthesis and sintering of mullite. *Ceram Int* 2009;**35**:3175–9.
15. Razavi-Hesabi Z, Haghighatzadeh M, Mazaheri M, Galusek D, Sadrnezhaad SK. Suppression of grain growth in sub-micrometer alumina via two-step sintering method. *J Eur Ceram Soc* 2009;**29**(8): 1371–7.
16. Mazaheri M, Razavi-Hesabi Z, Golestani-Fard F, Mollazadeh S, Jafari S, Sadrnezhaad SK. The effect of conformation method and sintering technique on the densification and grain growth of nanocrystalline 8 mol% yttria-stabilized zirconia. *J Am Ceram Soc* 2009;**92**(5):990–5.
17. Ghosh A, Suri AK, Rao BT, Ramamohan TR. Low-temperature sintering and mechanical property evaluation of nanocrystalline 8 mol% yttria fully stabilized zirconia. *J Am Ceram Soc* 2007;**90**(7):2015–23.
18. Wang J, Binner J, Vaidhyanathan B, Joomun N, Kilner J, Dimitrakis G, et al. Evidence for the microwave effect during hybrid sintering. *J Am Ceram Soc* 2006;**89**:1977–84.
19. Kuo CT, Chen CH, Lin IN. Microstructure and nonlinear properties of microwave-sintered $ZnO–V_2O_5$ varistors. II. Effect of Mn_3O_4 doping. *J Am Ceram Soc* 1998;**81**:2949–56.
20. Kuo CT, Chen CH, Lin IN. Microstructure and nonlinear properties of microwave-sintered $ZnO–V_2O_5$ varistors. I. Effect of V_2O_5 doping. *J Am Ceram Soc* 1998;**81**:2942–8.
21. Mazaheri M, Hesabi ZR, Sadrnezhaad SK. Two-step sintering of titania nanoceramics assisted by anatase-to-rutile phase transformation. *Scripta Mater* 2008;**59**(2):139–42.
22. Cottom MA, Mayo MJ. Fracture toughness of nanocrystalline ZrO_2–3 mol% Y_2O_3 determined by Vickers indentation. *Scripta Mater* 1996;**34**(5):809–14.